

R. Petre<sup>1</sup>, C.R. Canizares<sup>2</sup>, P.F. Winkler<sup>3</sup>, F.D. Seward<sup>4</sup>, R. Willingale<sup>5</sup>, D. Rolf<sup>5</sup>, and N. Woods<sup>5</sup>

<sup>1</sup>NAS/NRC Research Associate at Laboratory for High Energy Astrophysics, NASA/GSFC

<sup>2</sup>Center for Space Research, MIT; Alfred P. Sloan Foundation Fellow

<sup>3</sup>Middlebury College

<sup>4</sup>Harvard-Smithsonian Center for Astrophysics

<sup>5</sup>Leicester University

#### ABSTRACT

We present soft X-ray photomosaic images of two supernova remnants, Puppis A and IC 443, constructed from a series of exposures by the Einstein imaging instruments. The complex morphologies displayed in these images reflect the interaction between "middle-aged" supernova remnants and various components of the interstellar medium. Surface brightness variations across Puppis A suggest that inhomogeneities on scales from 0.2 to 30 pc are present in the interstellar medium, while the structure of IC 443 is apparently dominated by the interaction between the remnant and a giant molecular cloud.

In supernova remnants that have evolved well into their adiabatic expansion phase ( $t \sim 10^4$  yr), the bulk of the soft X-ray emission arises from recently shock-heated interstellar matter. The soft X-ray morphology of such "middle-aged" remnants will be influenced by any large or small scale inhomogeneities in the interstellar medium (ISM) they encounter. Consequently, these supernova remnants serve as excellent remote probes of the structure of the ISM.

We present and briefly discuss here high-resolution soft X-ray images of two such "middle-aged" remnants, Puppis A and IC 443. Despite their similarity in age ( $\sim 10^4$  yr), distance ( $\sim 2$  kpc) and diameter (25-30 pc), these two remnants display markedly different morphologies, presumably due largely to their different environments. A more extensive discussion of Puppis A may be found in Petre *et al.* (1982a); the IC 443 imaging results, along with spectral studies using the

289

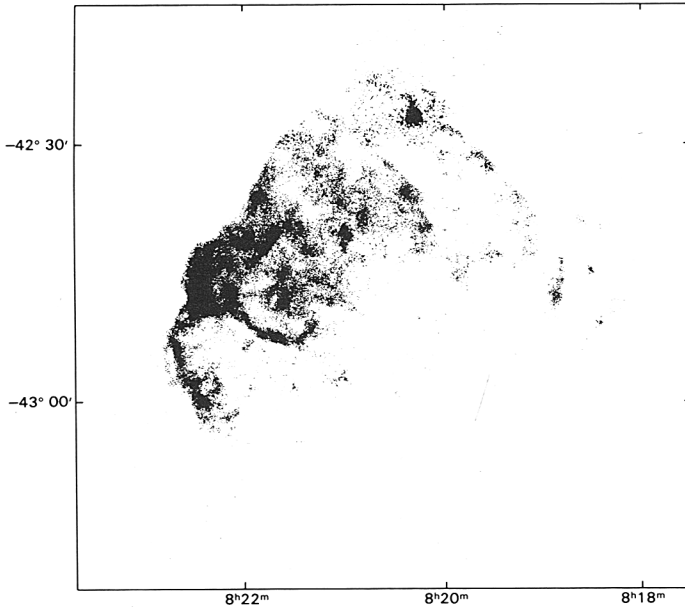


Figure 1: A high-resolution 0.1-4 keV photomosaic map of Puppis A.

appear in Petre et al. (1982b).

### Puppis A

Figure 1 shows a high-resolution X-ray image of Puppis A in the energy range 0.1-4.0 keV. The map is an exposure-corrected photomosaic of 11 Einstein High Resolution Imager (HRI) exposures, binned in 8" pixels. The image reveals an ISM with structure on many scales. First, there is a general decrease in X-ray surface brightness, by a factor of at least 20, from northeast to southwest across the remnant, perpendicular to the galactic plane. This effect is probably due to a local density gradient in the ISM of at least a factor of 4 over a scale of  $\sim 30$  pc. Second, the surface brightness variations in the interior and along the shell suggest a preshock ISM containing many small density variations (factors of 2), about an average of  $\sim 1 \text{ cm}^{-3}$ , over scales from 0.2 to 10 pc. Despite the surface brightness variations along the shell, the pronounced limb-brightening profiles are for the most part consistent with that expected for an adiabatically expanding blast wave, suggesting that the local clumpiness of the interstellar matter does not prevent the adiabatic model from being locally valid. Finally, in addition to the filamentary structure representing small density perturbations, Puppis A contains two bright knots of emission along the shell, one in the east and one in the northwest. These knots are probably shocked interstellar clouds with preshock density of 10-20  $\text{cm}^{-3}$  and diameter 1-2 pc.

IC 443

Figure 2 depicts a 0.2–3.1 keV map of IC 443, overlaid on a Palomar Sky Survey red plate. The map is an exposure-corrected, Wiener-filtered photomosaic of three Imaging Proportional Counter (IPC) images,

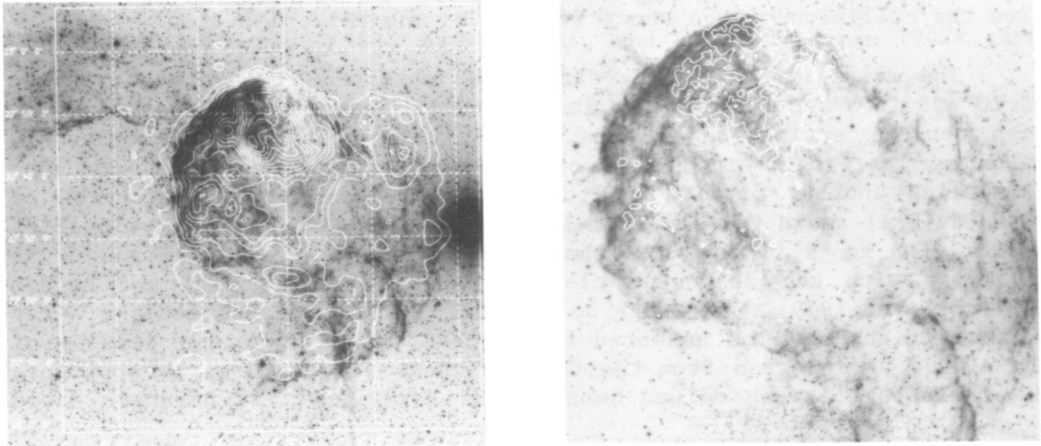


Figure 2 (left): A 0.2–3.1 keV image of IC 443, superposed on a Palomar Sky Survey red plate. This map is a photomosaic of three IPC images. Figure 3 (right): An HRI photomosaic of IC 443, superposed on the Palomar red plate.

binned in 32" pixels. The contours scale linearly with surface brightness. Although X-ray emission is detected from the entire SNR, the remnant does not appear to be limb-brightened. The average surface brightness in the vicinity of the bright northeastern optical filaments is a factor of  $\sim 4$  higher than elsewhere. This network of filaments has apparently been created by the collision of the shock front with a giant molecular cloud, which is observed in CO to extend well beyond IC 443 to the northeast (Scoville *et al.* 1977; Cornett, Chin and Knapp 1977).

A sharper view of the northern portion of IC 443 is shown in Figure 3. This map is an exposure-corrected, Wiener-filtered photomosaic of three HRI images, with 16" binning, whose coverage of IC 443 is represented approximately by the area over which the grid appears. The contour levels were chosen to reveal the highest X-ray surface brightness features; X-rays were actually detected by the HRI from everywhere in the complex of optical filaments, with the notable exception of the finger of optical extinction extending northeastward into the filaments.

The HRI map emphasises the dominant X-ray feature, a  $\sim 15'$  diameter region which partially overlaps the optical filaments. The pressure of the X-ray emitting gas in this region, as inferred from

spectral measurements by the Einstein SSS, is  $\sim 3 \times 10^{-9}$  dyne  $\text{cm}^{-2}$ , placing it in approximate equilibrium with the cooler, denser, optically-emitting gas (Fesen and Kirshner 1980). Coupled with the general overlap between the regions of high X-ray surface brightness and the bright northern optical filaments, this suggests that the X-ray emitting gas may be interspersed among the sites of unstable radiative cooling which appear as optical filaments, and that both have arisen from the collision of the shock front with the molecular cloud.

The molecular cloud may affect the observed low-energy structure of IC 443 in a second way. As is visible in Figures 2 and 3, a lane of high optical extinction bisects IC 443 from northwest to southeast, extending a finger into the bright optical filaments. This lane demarcates another portion of the molecular cloud. The detection of shocked [H I] and a variety of molecular species with typical velocities around  $-30 \text{ km s}^{-1}$  suggests that the front of the IC443 shell is colliding with the molecular cloud (see, e.g., Giovanelli and Haynes 1979; DeNoyer 1979). Although no general correlation between the X-ray surface brightness, as measured by the IPC, and the column density of the cloud, as inferred from the CO brightness temperature, is apparent, a correlation between column density and X-ray spectral hardness ratio

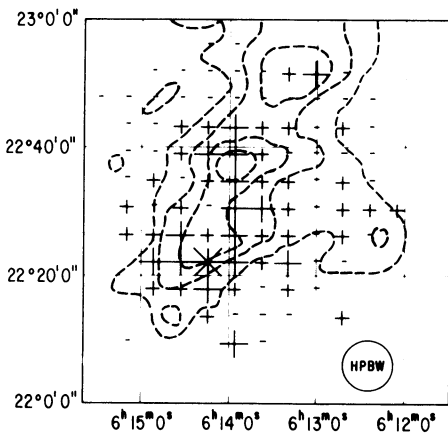


**Figure 4:** An IPC spectral hardness ratio map of IC 443, superposed on CO brightness temperature contours (from Cornett, Chin and Knapp 1977). Spectral hardness is defined as the ratio between 0.2-1.3 keV counts and 1.3-3.1 keV counts, with symbols of increasing prominence representing ratios of 0.6, 0.8, 1.0 and 1.2. Circle is HPBW of CO map.

(0.2-1.3 keV/1.3-3.1 keV) does exist. As seen in Figure 4, X-rays from regions coincident with the cloud are harder (average hardness ratio of  $\sim 0.8$ ) than elsewhere in the remnant (average hardness ratio of  $\sim 0.6$ ). To account for this increase of spectral hardness by absorption, a column density through the cloud of  $2-4 \times 10^{21} \text{ cm}^{-2}$  is required (in addition to the column density to IC 443) if the characteristic temperature of IC 443 is uniform and within the range of 0.5-1.5 keV. This additional column density may be compared to the inferred average column density of  $\text{H}_2$  through the cloud of  $2 \times 10^{21} \text{ cm}^{-2}$  (i.e.,  $4 \times 10^{21} \text{ cm}^{-2}$  of [H I] - Cornett, Chin and Knapp 1977). It is thus probable that the cloud absorbs X-rays emitted by the interior of IC 443.

## REFERENCES

- Cornett, R.H., Chin, G., and Knapp, G.R. 1977, *Astron. Ap.*, 54, pp. 889-894.
- DeNoyer, L.K. 1979, *Ap. J. (Letters)*, 228, pp. L41-L43.
- Fesen, R.A., and Kirshner, R.P. 1980, *Ap. J.*, 242, pp. 1023-1040.
- Giovanelli, R., and Haynes, M.P. 1979, *Ap. J.*, 230, pp. 404-414.
- Petre, R., Canizares, C.R., Kriss, G.A., and Winkler, P.F. 1982a, *Ap. J.*, 258, pp. 22-30.
- Petre, R., Szymkowiak, A.E., Canizares, C.R., Seward, F.D., Willingale, R., Rolf, D., and Woods, N. 1982b, in preparation.
- Scoville, N.Z., Irvine, W.M., Wannier, P.G., and Predmore, C.R. 1977, *Ap. J.*, 216, pp. 320-328.